ISBN: 978-3-95450-223-3 ISSN: 2673-7000 doi:10.18429/JACoW-NAPAC2019-MOPLH13

STARRE LAB: THE SUB-THZ ACCELERATOR RESEARCH LABORATORY*

J.F. Picard, S.C. Schaub, R.J. Temkin
Plasma Science and Fusion Center, Massachusetts Institute of Technology, Cambridge, MI, USA

Abstract

This work presents the development of the STARRE Lab, a facility at MIT for testing breakdown in high gradient accelerator structures at 110 GHz. The system utilizes a Laser-Driven Semiconductor Switch (LDSS) to modulate the output of a megawatt gyrotron, which generates 3 μs pulses at up to 6 Hz. The LDSS employs silicon (Si) and gallium arsenide (GaAs) wafers to produce nanosecond-scale pulses at the megawatt level from the gyrotron output. Photoconductivity is induced in the wafers using a 532 nm Nd:YAG laser, which produces 6 ns, 230 mJ pulses. A single Si wafer produces 110 GHz pulses with 9 ns width, while under the same conditions, a single GaAs wafer produces 24 ns 110 GHz pulses. In dual-wafer operation, which uses two active wafers, pulses of variable length down to 3 ns duration can be created at power levels greater than 300 kW. The switch has been successfully tested at incident 110 GHz RF power levels up to 720 kW. The facility has been used to successfully test an advanced 110 GHz accelerator structure built by SLAC to gradients in excess of 220 MV/m.

INTRODUCTION

With the potential for high efficiency in a small form factor, there has been growing interest in linear accelerator concepts driven at sub-THz and THz frequencies. Testing of these high-frequency structures requires RF pulses on the nanosecond timescale to avoid excessive pulsed heating. However, few sources exist that can achieve such short pulse widths at the required power levels. This paper presents a new test facility, the **S**ub-**T**erahertz **A**ccelerato**R** **RE**search Laboratory, or STARRE Lab, which utilizes a laser-driven semiconductor switch (LDSS) to produce megawatt-level, nanosecond-duration, sub-THz pulses to test advanced accelerator concepts. Previous experiments have documented LDSS behavior from microwave to the far-IR range but have been limited to the kilowatt power level [1]–[13]. The implementation of an LDSS with a megawatt-class gyrotron at 110 GHz, as in the STARRE Lab, represents a three order of magnitude increase in switched power over previous experiments and an exciting development in high-frequency accelerator testing capability. A full description of the behavior and testing of the LDSS has been published in [14].

FACILITY CAPABILITIES

Fig. 1 shows the setup of the STARRE Lab. A megawatt gyrotron produces 3 μs pulses of 110 GHz at up to 6 Hz. Each pulse has a flat-top power up to 1.5 MW [15]. The linearly-polarized output couples to the HE_{11} mode of a 31.75 mm diameter corrugated waveguide [16]. Power from the gyrotron can be continuously varied using a quasioptical microwave attenuator consisting of a half-waveplate and five quartz plates at the Brewster angle. Microwaves then enter a laser enclosure containing the LDSS.

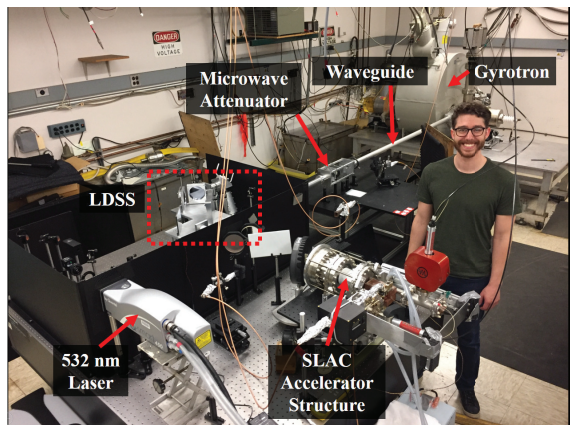

Figure 1: The STARRE Lab. A 1.5 MW, 110 GHz, gyrotron provides the input pulse to the LDSS, which is contained within a laser enclosure at center. The LDSS produces a shortened pulse, which exits the enclosure into the accelerator test stand (see Fig. 3).

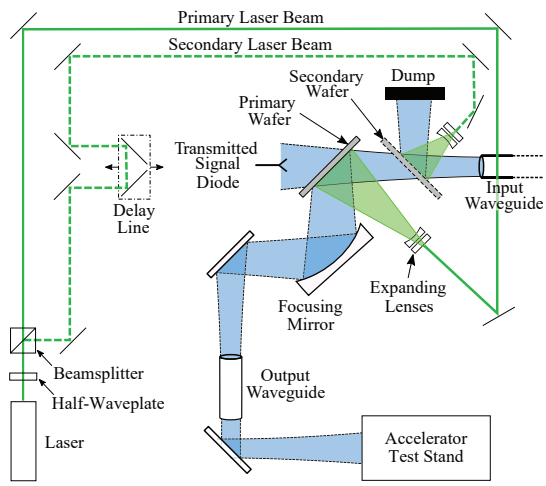

Figure 2: Experimental setup of the LDSS which feeds the accelerator test stand. 110 GHz microwaves generated by the MIT megawatt gyrotron are in blue and enter the setup from the input waveguide. Laser beams are shown in green.

A functional schematic of the LDSS system in the STARRE Lab can be seen in Fig. 2. 110 GHz radiation

* jpicard@mit.edu

ISBN: 978-3-95450-223-3 ISSN: 2673-7000 doi:10.18429/JACoW-NAPAC2019-MOPLH13

from the gyrotron enters the LDSS from the input waveguide. Because of small reflections returning to the gyrotron, the maximum power into the LDSS is currently limited to 720 kW. The LDSS is configured for both single- and dual-wafer operation. In single-wafer operation, only the primary wafer and primary laser beam are active. Both the GaAs and Si wafers used are initially transparent to the 110 GHz signal from the gyrotron, absorbing <0.1% of the incident RF power. When a laser is incident upon the primary semiconductor wafer with a frequency such that the photon energy is greater than the band gap energy, free carriers are generated within the wafer. The population of these carriers, n, can be treated as an electron-hole plasma with plasma frequency $\omega_{RF} = \sqrt{e^2 n/m_e \epsilon_0}$, where m_e is the electron mass, e is the fundamental charge, and ϵ_0 is the vacuum permittivity. When the plasma frequency increases above 110 GHz the primary wafer becomes reflective, redirecting the RF beam to the output stage. The reflection persists for a period determined by the laser pulse parameters and the wafer recombination effects. Dual-wafer operation allows for active truncation of the output pulse by using a second wafer and laser beam. At a time Δt after the primary wafer is illuminated, the secondary wafer is illuminated by the secondary laser beam. The secondary wafer then reflects the 110 GHz from the input waveguide into a dump, which truncates the output pulse to a width of Δt. An optical delay line allows for the free adjustment of Δt. In either mode, the subsequent chopped output pulse exits the laser enclosure through a short corrugated waveguide.

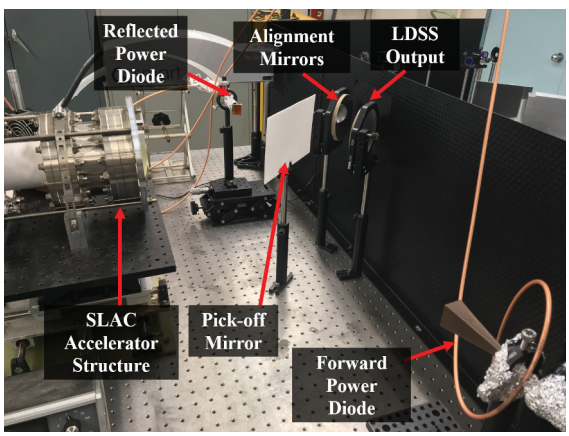

Figure 3: Accelerator test stand at the output of the LDSS.

The LDSS output waveguide feeds the accelerator test stand, seen in Fig. 3. Two mirrors allow for transverse alignment, and a pick-off mirror is employed to sample both the forward pulse and any reflected pulse from the structure under test. In Fig. 3, an accelerator structure developed by SLAC (discussed later) is mounted on a 3-axis lab jack for longitudinal alignment as well as additional freedom during transverse alignment.

The 532 nm, ~6 ns, laser pulse used to induce photoconductivity is produced by a Quantel Q-smart 450 with a frequency doubling stage, pictured at bottom left in Fig. 1. This wavelength was chosen such that the photon energy, 2.33 eV, exceeds the band gap energy of Si (1.11 eV) and GaAs (1.43 eV) by a substantial margin. The maximum energy per pulse of 230 mJ can be divided between the primary and secondary laser beams with a half-waveplate and polarizing beamsplitter. A representative 215 mJ laser pulse can be seen in Fig. 4a. On the wafer surface, the peak laser intensity is 3.5 MW/cm^2 and the total energy density is 15.3 mJ/cm^2. The structure of the laser pulse is caused by longitudinal modes in the laser cavity.

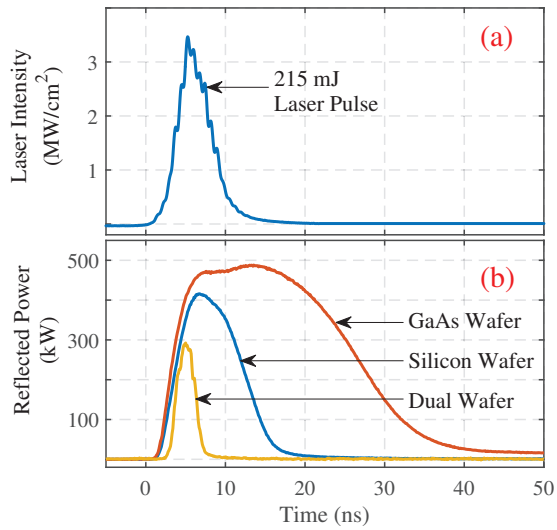

Figure 4: (a) Experimentally measured temporal profile of the 532 nm laser pulse used to excite the Si and GaAs wafers. (b) Characteristic reflected pulses from the GaAs wafer (red) and Si wafer (blue) in single wafer operation, with 525 kW incident 110 GHz RF power and 215 mJ incident laser energy. Dual wafer operation is in yellow, with Si as the primary wafer (illuminated by 120 mJ of laser energy), and GaAs as the secondary wafer (illuminated by 100 mJ of laser energy). Adjusting the optical delay line (see Fig. 2) allows for continuous variation of the dual-wafer pulse width [14].

Fig. 4b features representative 110 GHz pulses produced by the LDSS in both single- and dual-wafer mode, tested at 525 kW of incident 110 GHz power. The incident 525 kW, 110 GHz pulse from the gyrotron (not shown) is 3 μs in duration. In single-wafer mode, a Si wafer produces a 9 ns reflected pulse with a peak power of 410 kW, corresponding to 78% of the input power. A GaAs wafer under the same conditions produces a 24 ns pulse with a peak power of 485 kW, corresponding to 92% of the incident 110 GHz beam. The rise time of the reflected RF pulse is dictated by the laser rise time, which can be seen by comparing the output pulses in Fig. 4b with the pulse from the laser, Fig. 4a. In single wafer operation, the fall time is dominantly set by the recombination timescale of the electron-hole plasma within the wafer. This can be seen most strongly in the GaAs trace, for which maximum reflection persists for ~10 ns after peak

ISBN: 978-3-95450-223-3 ISSN: 2673-7000 doi:10.18429/JACoW-NAPAC2019-MOPLH13

laser intensity before decaying to negligible levels ~30 ns later. In dual-wafer mode, the pulse width at the output can be continuously varied with the optical delay line to produce pulses such as the 3 ns dual-wafer pulse in Fig. 4b, with a peak 110 GHz power of 300 kW. Pulses with 650 kW of peak power have been achieved, and tests using alternative wafers with longer recombination times (not shown) produced up to 3 μs pulses, which is the maximum created by the megawatt gyrotron.

PHYSICS RESULTS

During the development of the STARRE Lab, experiments were conducted to measure the reflectance of the Si and GaAs wafers as a function of incident laser and 110 GHz intensity. The results of these experiments can be seen in Fig. 5. The characteristic "saturation" behavior of the curves has been observed extensively in previous experiments [7], [13], [17]. The curves corresponding to the GaAs wafer exhibit a clear saturation around 8 mJ/cm^2, while the Si wafer does not reach saturation even at maximum laser energy density (15.3 mJ/cm^2, 215 mJ total). This may indicate that additional laser power would be required to achieve saturation of the Si wafer. Fig. 5 also demonstrates our finding that at high incident microwave power the peak reflectance of both Si and GaAs wafers increases. At the peak laser energy density of 15.3 mJ/cm^2 and low RF intensity (25 kW total power) the GaAs wafer has a reflectance of 81 ± 2%. At high RF intensity (480 kW total power), however, the GaAs wafer reflectance increases to 90 ± 2%. Under the same conditions, the Si wafer has a reflectance of 72±2% at lower RF intensity, which increases to 80±2% at high RF intensity. This increase in reflectance may be due to absorbed energy from the high-intensity 110 GHz pulse. In these experiments, the 480 kW pulse of 110 GHz corresponds to a peak RF intensity on the wafer of 0.095 MW/cm^2.

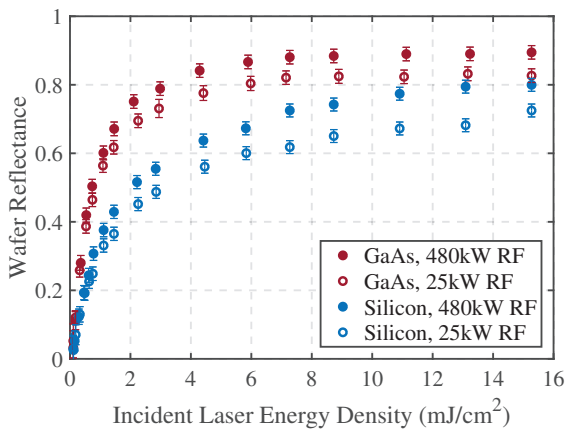

Figure 5: Peak reflectance vs. laser energy density for GaAs and Si wafers at low (25 kW) and high (480 kW) incident 110 GHz power. Maximum laser energy density of 15.3 mJ/cm^2 corresponds to 215 mJ total incident laser energy [14].

A high-frequency accelerator test cavity developed by SLAC is currently undergoing high-power testing at the STARRE Lab. The 110 GHz single-cell standing wave accelerator cavity is designed to measure RF breakdown probability and can be seen installed in Figs. 1 and 3. Fig. 6 shows forward, transmitted, and reflected power traces from high-power testing of the structure. The traces were collected with 575 kW of input power, corresponding to >220 MV/m accelerating gradient. Additional details regarding this experiment are available in [18].

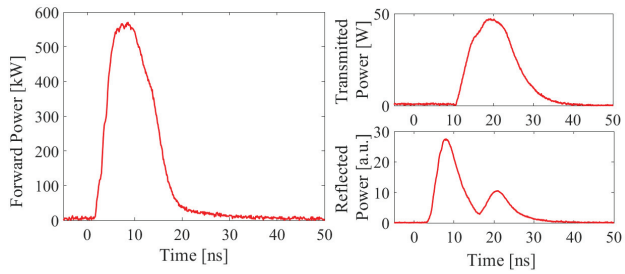

Figure 6: Sample forward, transmitted, and reflected traces from high-power testing of the SLAC accelerator concept, from [18], corresponding to >220 MV/m accelerating gradient.

CONCLUSION

Through the implementation of a laser-driven semiconductor switch with a megawatt gyrotron at 110 GHz, the STARRE Lab enables the testing of advanced, high-frequency accelerator concepts with a high degree of tunability in both power and pulse width. Pulse widths from <3 ns to 3 μs have been generated at continuously-variable power levels up to 650 kW. Ongoing testing of a SLAC high-frequency accelerator structure at the STARRE Lab has produced accelerating gradients of greater than 220 MV/m.

ACKNOWLEDGMENTS

This work was supported by the Department of Energy, Office of High Energy Physics under grant No. DE-SC0015566, the Office of Fusion Energy Sciences through grant No. DE-FC02-93ER54186, and by the National Institutes of Health, National Institute for Biomedical Imaging and Bioengineering under Grant EB004866 and Grant EB001965.

REFERENCES

[1] M. L. Kulygin, V. I. Belousov, G. G. Denisov, A. A. Vikharev, V. V. Korchagin, A. V. Kuzin, E. A. Novikov, and M. A. Khozin, "Development of waveguide semiconductor switches of microwave radiation in the 70- and 260-ghz ranges," *Radiophys. Quantum Electron.*, vol. 57, no. 7, p. 509, Dec. 2014. DOI: 10.1007/s11141-014-9533-6.

ISBN: 978-3-95450-223-3 ISSN: 2673-7000 doi:10.18429/JACoW-NAPAC2019-MOPLH13

[2] S. Mitsudo, C. Umegaki, Y. Fujii, and Y. Tatematsu, "Quasi-optical transmission system for a pulsed esr system by using a gyrotron as a light source," in *Proc. IEEE 40th Int. Conf. Infrared Millim. Terahertz Waves, Hong Kong, China*, Aug. 2015, p. 1. DOI: 10.1109/IRMMW-THz.2015.7327943.

[3] D. H. Auston, "Picosecond optoelectronic switching and grating in silicon," *Appl. Phys. Lett.*, vol. 26, no. 3, p. 101, 1975. DOI: 10.1063/1.88079.

[4] M. S. Choe, A. Sawant, K.-S. Lee, N. E. Yu, and E. Choi, "Measuring the carrier lifetime by using a quasi-optical millimeter- and thz-wave system," *Appl. Phys. Lett.*, vol. 110, no. 7, p. 074 101, 2017. DOI: 10.1063/1.4976315.

[5] G. Mourou, C. V. Stancampiano, A. Antonetti, and A. Orszag, "Picosecond microwave pulses generated with a subpicosecond laser-driven semiconductor switch," *Appl. Phys. Lett.*, vol. 39, no. 4, p. 295, 1981. DOI: 10.1063/1.92719.

[6] C. H. Lee, "Picosecond optoelectronic switching in gaas," *Appl. Phys. Lett.*, vol. 30, no. 2, p. 84, 1977. DOI: 10.1063/1.89297.

[7] S. Takahashi, L. Brunel, D. T. Edwards, J. van Tol, G. Ramian, S. Han, and M. S. Sherwin, "Pulsed electron paramagnetic resonance spectroscopy powered by a free-electron laser, supplementary information," *Nature*, vol. 489, p. 409, 2012. DOI: 10.1038/nature11437.

[8] F. A. Hegmann and M. S. Sherwin, "Generation of picosecond far-infrared pulses using laser-activated semiconductor reflection switches," in *Proc. SPIE 2842, Millimeter and Submillimeter Waves and Applications III,*, 1996, p. 90. DOI: 10.1117/12.262736.

[9] K. Kawase, R. Kato, A. Irizawa, M. Fujimoto, K. Furukawa, K. Kubo, and G. Isoyama, "Single picosecond thz pulse extraction from the fel macropulse using a laser activating semiconductor reflective switch," in *Proc. 37th Int. Free Electron Laser Conference (FEL 2015), Daejeon, Korea*, Dec. 2015, p. 430. DOI: 10.18429/JACoW-FEL2015-TUP029.

[10] M. Kulygin, "Stress test of nanosecond semiconductor cavity switches with subterahertz gyrotrons," *IEEE Trans. Terahertz Sci. Technol.*, vol. 9, p. 186, 2019. DOI: 10.1109/TTHZ.2019.2891020.

[11] M. Rahm, J. Li, and W. J. Padilla, "Thz wave modulators: A brief review on different modulation techniques," *J. Infrared Millim. Terahertz Waves*, vol. 34, no. 1, p. 1, Jan. 2013, ISSN: 1866-6906. DOI: 10.1007/s10762-012-9946-2.

[12] A. Woldegeorgis, T. Kurihara, B. Beleites, J. Bossert, R. Grosse, G. G. Paulus, F. Ronneberger, and A. Gopal, "Thz induced nonlinear effects in materials at intensities above 26 gw/cm2," *J. Infrared Millim. Terahertz Waves*, vol. 39, no. 7, p. 667, Jul. 2018. DOI: 10.1007/s10762-018-0493-3.

[13] T. Nozokido, H. Minamide, and K. Mizuno, "Modulation of submillimeter wave radiation by laser-produced free carriers in semiconductors," *Electron Comm. Jpn. Part 2*, vol. 80, p. 259, 1997. DOI: 10.1002/(SICI)1520-6432(199706)80:6<1::AID-ECJB1>3.0.CO;2-P.

[14] J. F. Picard, S. S. C., G. Rosenzweig, J. Stephens, M. A. Shapiro, and R. J. Temkin, "Laser-driven semiconductor switch for generating nanosecond pulses from a megawatt gyrotron," *Appl. Phys. Lett.*, vol. 114, no. 164102, 2019. DOI: 10.1063/1.5093639.

[15] E. M. Choi, C. D. Marchewka, I. Mastovsky, J. R. Sirigiri, M. A. Shapiro, and R. J. Temkin, "Experimental results for a 1.5mw, 110ghz gyrotron oscillator with reduced mode competition," *Phys. Plasmas*, vol. 13, no. 2, p. 023 103, 2006. DOI: 10.1063/1.2171522.

[16] J. M. Neilson, R. L. Ives, S. C. Schaub, W. C. Guss, G. Rosenzweig, R. J. Temkin, and P. M. Borchard, "Design and high-power test of an internal coupler to he11mode in corrugated waveguide for high-power gyrotrons," *IEEE Trans. Electron Devices*, vol. 65, p. 2316, 2018. DOI: 10.1109/TED.2018.2805889.

[17] M. Kulygin, G. Denisov, K. Vlasova, N. Andreev, S. Shubin, and S. Salahetdinov, "Sub-terahertz microsecond optically controlled switch with gaas active element beyond the photoelectric threshold," *Rev. Sci. Instrum.*, vol. 87, p. 014 704, Jan. 2016. DOI: 10.1063/1.4939673.

[18] M. A. K. Othman, J. Picard, S. Schaub, V. Dolgashev, S. Jawla, B. Spataro, R. J. Temkin, S. Tantawi, and E. A. Nanni, "High-gradient test results of w-band accelerator structures," in *2019 44th International Conference on Infrared, Millimeter, and Terahertz Waves (IRMMW-THz), Paris, 2019*, Sep. 2019, p. 1.